DOI: 10.1002/ejic.200900890

Mononuclear Platinum(II) Complexes of a Bis(bidentate) Ligand Based on 1,3,4-Oxadiazole and Their Reactions with Copper(I) Salts

Marc-Etienne Moret[a] and Peter Chen*[a]

Keywords: Platinum / Copper / N ligands / Metal–metal interactions / Bridging ligands

Reaction of the bis(bidentate) ligand 2,5-bis[2-(dimethylamino)phenyl]-1,3,4-oxadiazole (oxanMe) with the precursors *trans*-[PtMeCl(SMe$_2$)$_2$] and [(PhCN)$_2$PtCl$_2$] afforded the mononuclear complexes [(oxanMe)Pt(Me)Cl] and [(oxanMe)-PtCl$_2$], respectively. [(oxanMe)PtMe$_2$] was observed in equilibrium with oxanMe, [Pt$_2$Me$_4$(μ-SMe$_2$)$_2$], and [PtMe$_2$-(SMe$_2$)$_2$], but could not be isolated. Reaction of [(oxanMe)-PtCl$_2$] with silver acetate gave access to [(oxanMe)Pt(OAc)$_2$] in excellent yield. The latter was treated with [Cu(NCMe)$_4$]-BArF, resulting in a disproportionation reaction that afforded the novel trimetallic complex {[(oxanMe)Pt(OOCCH$_3$)$_2$]$_2$-Cu}{BArF}$_2$. This complex features a linear Pt^{II}–Cu^{II}–Pt^{II} chain consisting of two Pt→Cu dative bonds supported by two bridging acetate ligands each.

Introduction

Complexes of platinum(II) with chelating, N-donor ligands have attracted a lot of interest in the last decade due to their use as precursors for C–H bond activation of unreactive substrates.[1–10] In particular, complexes incorporating a methyl ligand are useful because the transient Pt^{IV} hydrides formed by oxidative addition of a C–H bond can then reductively eliminate methane, which drives the reaction to completion.[11–23] Some Pt^{II} carboxylate complexes have also been shown to be active benzene deuteration catalysts.[5,24,25] In search for novel reactivity related to C–H bond activation, we recently became interested in polynuclear complexes incorporating platinum and copper centers in close proximity.[26,27]

Incarvito et al. recently introduced a class of N-donor, dinucleating ligands based on a 1,3,4-oxadiazole bridging unit and showed that these could be used to form dinuclear compounds.[28,29] The simplest member and common precursor of this family is the ligand oxanH (**1**; Scheme 1). In this contribution, we present the synthesis of its tetramethylated derivative, oxanMe (**2**), and explore the coordination chemistry of **2** with common Pt^{II} precursors, showing that it preferentially forms mononuclear Pt^{II} complexes. Reaction of these complexes with [Cu(NCMe)$_4$]$^+$ salts does not allow the isolation of the desired heterobimetallic complexes, but in one case a novel trimetallic complex exhibiting an acetate-supported Pt^{II}–Cu^{II}–Pt^{II} chain can be isolated and characterized by single crystal X-ray diffraction (XRD).

[a] Laboratorium für Organische Chemie, Eidgenössische Technische Hochschule (ETH) Zürich,
8093 Zürich, Switzerland
Fax: +41-44 632 15 92
E-mail: peter.chen@org.chem.ethz.ch

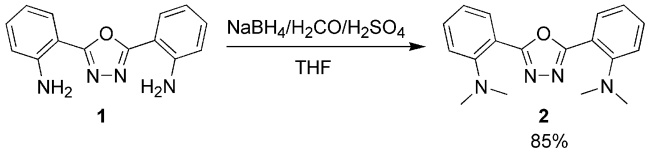

Scheme 1. Synthesis of oxanMe (**2**).

Results and Discussion

Ligand **2** was synthesized in 85% yield by tetramethylation of **1** by using the method of Giumanini et al.[30] for the selective dimethylation of anilines (Scheme 1). This procedure relies on the condensation of the aniline functionality with formaldehyde to form transient iminium cations that are subsequently hydrogenated by NaBH$_4$.

The reaction of ligand **2** with the precursor [Pt$_2$Me$_4$(μ-SMe$_2$)$_2$] proceeded over a few minutes to form new complex **3** [Scheme 2, reaction (I)]. However, this reaction did not run to completion, but reached equilibrium at ca 35% conversion (based on the amount of **2**). The ^{1}H NMR spectrum of **3** exhibits eight aromatic signals, two signals corresponding to NMe$_2$ moieties and two different Pt–Me signals, in accord with the formulation of **3** as the mononuclear complex [(oxanMe)PtMe$_2$]. Furthermore, the fact that one of the NMe$_2$ moieties in **3** is coordinated to the platinum center is evident from the appearance of platinum satellites ($^3J_{H,Pt}$ = 14.0 Hz) around the corresponding methyl hydrogen signal.

Several attempts were made to shift the equilibrium by selective crystallization or removal of dimethyl sulfide under low pressure, but isolation of **3** remained elusive, partly due to the moderate stability of [Pt$_2$Me$_4$(μ-SMe$_2$)$_2$] in solution. In a related experiment, the reaction was performed in the presence of CuBr, with the hope that SMe$_2$ would be

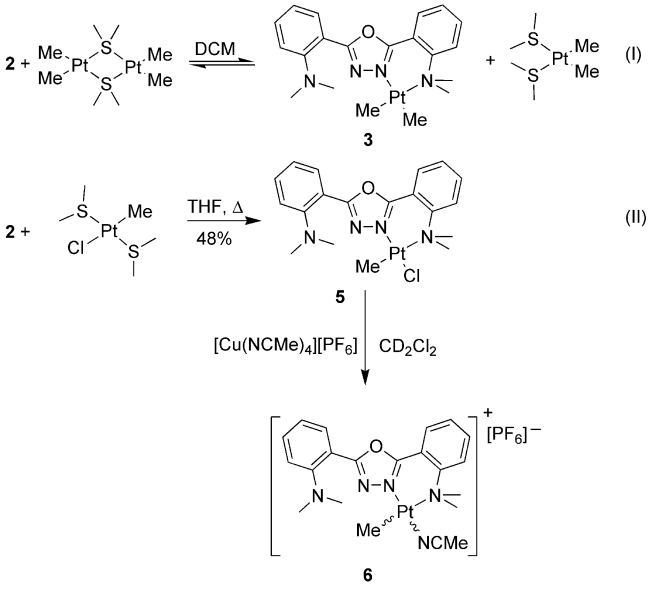

Scheme 2. Reactions of **2** with methylplatinum(II) precursors.

withdrawn from the solution by formation of the poorly soluble solid $CuBr{\cdot}SMe_2$. However, CuBr was solubilized by interaction with **2** and only the complex $[(oxanMe)_2Cu_4Br_4]$ (**4**) could be isolated from the reaction mixture.

XRD analysis of **4** (Figure 1) revealed a C_2-symmetrical $(CuBr)_4$ cycle stabilized by N,N chelation of all four copper(I) centers. Each metal has a distorted tetrahedral environment, with large Br–Cu–Br angles [132.26(3) and 115.87(3)°] and acute N–Cu–N bite angles [80.79(15) and 81.35(15)°]. The Cu–N bonds involving the oxadiazole unit are remarkably shorter than those involving the NMe_2 moiety [2.024(4) and 1.994(4) Å vs. 2.434(4) and 2.434(5) Å], indicating that the former are stronger donors, even though the oxadiazole ring acts as a bridge between two metals. The rare $(CuBr)_4$ cycle found in **4** is similar to that reported by Filinchuk et al.[31] in the complex $\{[1\text{-(fur-2-yl)-2-azapenta-1,4-diene}]_2Cu_4Br_4\}$.

A methylplatinum(II) complex of **2** was obtained by reaction with the more robust precursor $[(SMe_2)_2Pt(Me)Cl]$, which yielded complex **5** in 48% yield [Scheme 2, reaction (II)] as a single stereoisomer that was identified by XRD (Figure 2). In the crystal structure of **5**, the platinum(II) center experiences only a slightly distorted square planar environment, the bite angle of oxanMe [85.1(2)°] being close to the ideal 90°. The Pt1–N1 bond is markedly longer than Pt1–N2 [2.256(7) vs. 1.990(5) Å], which is due both to the weaker σ-donor character of N1 and to the stronger *trans*-influence of the methyl ligand as compared to chloride.

Reaction of **5** with $[Cu(NCMe)_4][PF_6]$ did not result in the formation of a dinuclear complex. In contrast, the chloride ligand was abstracted by precipitation of CuCl, resulting in the formation of cationic complex **6** (Scheme 2), which was identified by ^1H NMR spectroscopy and mass spectrometry (ESI). Isolation of **6** was not attempted.

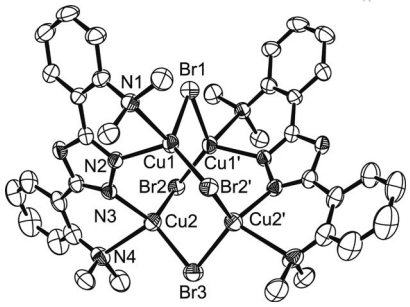

Figure 1. ORTEP representation of **4**. Ellipsoids are drawn at 50% probability. Four CH_2Cl_2 molecules are omitted for clarity. Selected distances [Å], angles [°], and torsion angles [°]: Cu1–N1 2.434(4), Cu1–N2 2.024(4), Cu1–Br1 2.4120(9), Cu1–Br2′ 2.3650(8), Cu2–N3 1.994(4), Cu2–N4 2.434(5), Cu2–Br2 2.4345(9), Cu2–Br3 2.3656(9), N1–Cu1–N2 80.79(15), N1–Cu1–Br1 97.57(11), N1–Cu1–Br2′ 101.17(11), N2–Cu1–Br1 107.10(13), N2–Cu1–Br2′ 118.98(13), Br1–Cu1–Br2′ 132.26(3), N3–Cu2–N4 81.35(16), N3–Cu2–Br2 106.96(13), N3–Cu2–Br3 134.39(13), N4–Cu2–Br2 102.33(13), N4–Cu2–Br3 103.28(13), Br2–Cu2–Br3 115.87(3), Cu1–Br1–Cu1′ 79.79(4), Cu1–Br2′–Cu2′ 90.63(3), Cu2–Br3–Cu2′ 86.42(4), Cu1–N2–N3–Cu2 1.7(5).

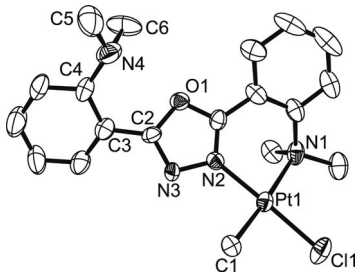

Figure 2. ORTEP representation of **5**. Ellipsoids are drawn at 50% probability. Selected distances [Å], angles [°], and torsion angles [°]: Pt1–C1 2.039(8), Pt1–Cl2 2.2830(19), Pt1–N1 2.256(7), Pt1–N2 1.990(5), C1–Pt1–Cl2 88.4(2), C1–Pt1–N2 90.8(3), Cl1–Pt1–N1 95.69(16), N1–Pt1–N2 85.1(2), Pt1–N2–N3 125.9(4), N3–C2–C3–C4 155.4(7), C3–C4–N4–C5 –147.3(8), C3–C4–N4–C6 92.1(9).

Platinum(II) diacetate complex **9** was accessed in two steps from ligand **2**. First, dichlorido complex **7** was obtained by heating **2** at reflux with $[(PhCN)_2PtCl_2]$ in THF for 68 h, during which time **7** (83%) precipitated in analytical purity (Scheme 3). Upon storage of the liquid phase for several days, a byproduct crystallized as pale-yellow needles, which were identified as bi-oxanMe complex **8**. Complex **7** was then treated with silver acetate to yield diacetato complex **9** in excellent yield (Scheme 3). Complexes **7**, **8**, and **9** were subjected to XRD analysis.

Two different polymorphic structures **A** and **B** (Figure 3) were obtained by recrystallization of **7** from acetonitrile and dichloromethane/diethyl ether, respectively. The molecular units in **A** and **B** differ mainly by a rotation around the C4–C5 bond, with N3–C4–C5–C6 dihedral angles of 153(8) and –12.6(10)°, respectively. In both cases, the geometry around the platinum atom is square planar, with bite angles of 86.5(2) and 86.20(18)°. Despite the fact that both nitrogen atoms are located *trans* to a chloride ligand, the Pt1–N1 bond is considerably longer than Pt1–N2 [**A**: 2.142(5) vs.

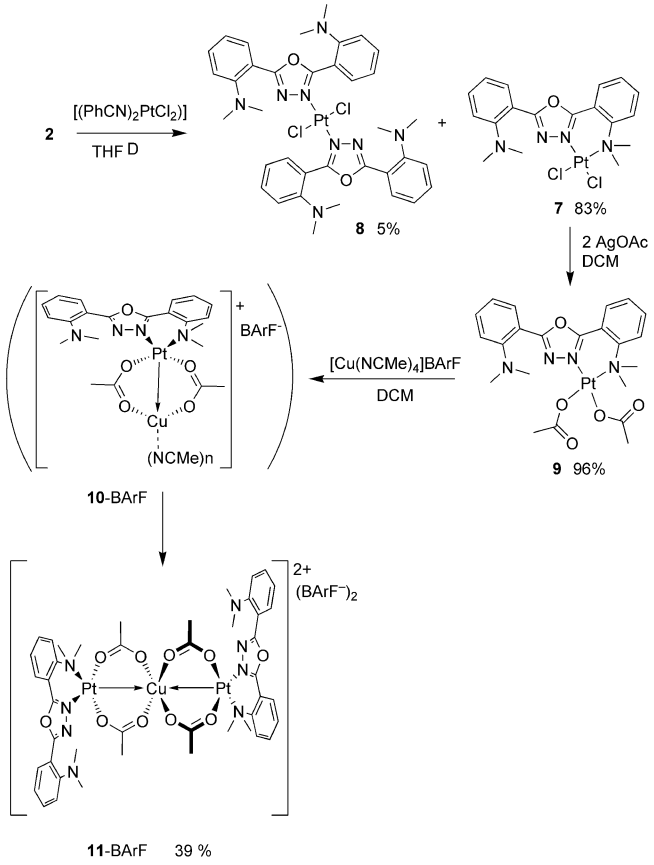

Scheme 3. Synthesis of [(oxanMe)Pt(OAc)$_2$] (**9**) and its reaction with [Cu(NCMe)$_4$]BArF {BArF = tetrakis[3,5-bis(trifluoromethyl)-phenyl]borate}.

2.005(5) Å; **B**: 2.135(5) vs. 2.003(4) Å]. This indicates that the Pt–N1 interaction is weaker than Pt–N2, in accord with the observation that both oxanMe units are coordinated through N2 in the 2:1 byproduct **8** (Figure 4).

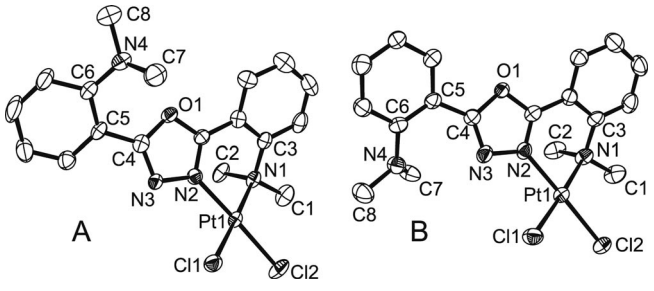

Figure 3. ORTEP representations of the two different structures found for **7**. Ellipsoids are drawn at 50% probability. Selected distances [Å], angles [°], and torsion angles [°]: For structure **A**: Pt1–Cl1 2.2929(15), Pt1–Cl2 2.2838(15), Pt1–N1 2.142(5), Pt1–N2 2.005(5), Cl1–Pt1–Cl2 87.96(6), Cl1–Pt1–N2 90.53(15), Cl2–Pt1–N1 95.06(14), N1–Pt1–N2 86.5(2), Pt1–N2–N3 128.0(4), N3–C4–C5–C6 153.8(6), C5–C6–N4–C7 125.4(8), C5–C6–N4–C8 –56.6(9); for structure **B**: Pt1–Cl1 2.2905(15), Pt1–Cl2 2.2904(13), Pt1–N1 2.135(5), Pt1–N2 2.003(4), Cl1–Pt1–Cl2 88.20(5), Cl1–Pt1–N2 90.46(14), Cl2–Pt1–N1 95.15(13), N1–Pt1–N2 86.20(18), Pt1–N2–N3 127.0(4), N3–C4–C5–C6 –12.6(10), C5–C6–N4–C7 164.6(6), C5–C6–N4–C8 –47.2(8).

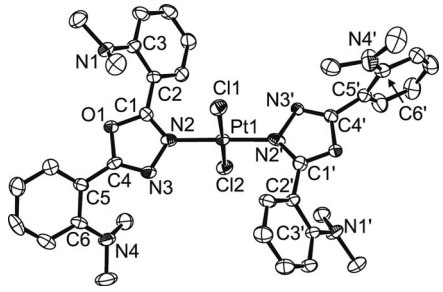

Figure 4. ORTEP representation of **8**. Ellipsoids are drawn at 50% probability. Selected distances [Å], angles [°], and torsion angles [°] (values for the right-most oxanMe ligand in square brackets): Pt1–Cl1 2.2982(18), Pt1–Cl2 2.2915(18), Pt1–N2 1.971(6) [1.974(6)], Cl1–Pt1–N2 90.02(17) [88.89(18)], Cl2–Pt1–N2 88.44(17) [92.69(18)], Pt1–N2–N3 120.5(4) [121.2(4)], Cl1–Pt1–N2–N3 –102.9(5) [–84.3(5)], N2–C1–C2–C3 –138.8(8) [132.8(8)], N3–C4–C5–C6 –36.3(12) [95.9(10)].

The XRD structure of **8** exhibits a square-planar geometry around Pt^{II}. The two oxanMe units are bound to platinum through the oxadiazole units, which are approximately perpendicular to the coordination plane, with Cl1–Pt1–N2–N3 and Cl1–Pt1–N2′–N3′ dihedral angles of –102.9(5) and –84.3(5)°, respectively. The N-donor ligands are in a *trans* position, which is likely due to steric repulsion between them.

The unit cell of **9** contains two crystallographically independent molecules (Figure 5) that differ by the conformation of the exocyclic C–C bond [N3–C3–C4–C5 dihedral angles of 157.9(6) and –5.1(10)°, respectively]. In both molecules, the acetate ligands are bound in a *syn* fashion, that is, the Pt1–O1–C1–O3 [–3.4(8), 15.8(8)°] and Pt1–O2–C2–O4 [6.2(9), –5.9(8)°] dihedral angles have values close to 0, and their uncoordinated oxygen atoms are on opposite sides of the coordination plane.

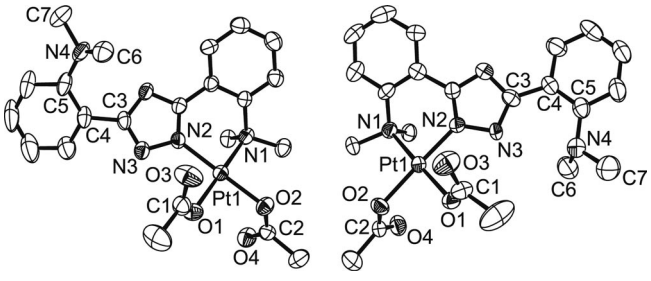

Figure 5. ORTEP representations of the two crystallographically different molecules found in the unit cell of **9**. Ellipsoids are drawn at 50% probability. For clarity, one molecule of diethyl ether present in the unit cell is omitted. Selected distances [Å], angles [°], and torsion angles [°] for the molecule plotted on the left [right]: Pt1–O1 2.004(4) [2.021(4)], Pt1–O2 2.028(4) [2.026(4)], Pt1–N1 2.097(5) [2.114(5)], Pt1–N2 1.980(4) [1.969(4)], O1–C1 1.267(7) [1.274(8)], C1–O3 1.220(7) [1.232(7)], O2–C2 1.274(7) [1.287(7)], C2–O4 1.222(6) [1.224(7)], O1–Pt1–O2 85.98(16) [85.80(16)], O1–Pt1–N2 92.33(18) [91.01(17)], O2–Pt1–N1 94.63(17) [95.63(17)], N1–Pt1–N2 87.35(18) [87.68(18)], Pt1–O1–C1 119.1(4) [118.1(4)], Pt1–O2–C2 118.4(3) [120.7(3)], Pt1–O1–C1–O3 –3.4(8) [15.8(8)], Pt1–O2–C2–O4 6.2(9) [–5.9(8)], N3–C3–C4–C5 157.9(6) [–5.1(10)], C4–C5–N4–C6 –53.0(9) [69.0(7)], C4–C5–N4–C7 167.3(6) [–161.6(6)].

The interaction of **9** with copper(I) was studied by ESI-MS analysis of a dichloromethane solution containing equimolar amounts of **9** and [Cu(NCMe)$_4$]BArF (BArF = tetrakis[3,5-bis(trifluoromethyl)phenyl]borate). The obtained spectrum features one main peak at *m*/*z* = 685, which is assigned to the 1:1 complex [(oxanMe)Pt(OAc)$_2$Cu]$^+$ (**10**$^+$) on the basis of its isotope pattern (Figure 6). Upon collision-induced dissociation (CID), it loses either acetic acid or a molecule of copper(I) acetate, in accord with its assignment.

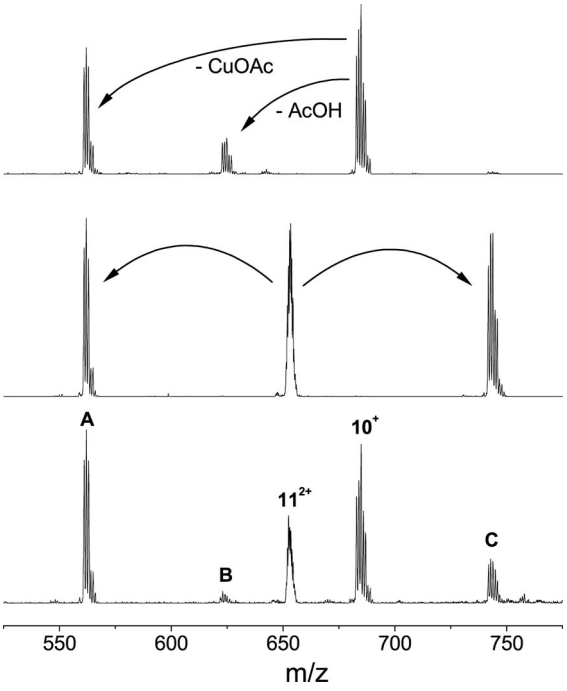

Figure 6. Bottom: ESI mass spectrum of a solution of **9** and [Cu(NCMe)$_4$]BArF 1 d after preparation, showing cations **10**$^+$ and **11**$^{2+}$ together with their fragmentation products. Middle: CID spectrum of **11**$^{2+}$. Top: CID spectrum of **10**$^+$. Peak assignment: **A**: [(oxanMe)Pt(OAc)]$^+$; **B**: **10**$^+$ – AcOH; **C**: [(oxanMe)PtCu(OAc)$_3$]$^+$.

Because mass spectrometry provides no structural information, the structure of **10**$^+$ was investigated by density functional theory (DFT) calculations at the BP86/6-31+G(d);Pt,Cu:SDD level, which we have previously shown to yield reliable geometries and energies for related Pt–Cu mixed complexes.[27] We optimized the geometries of the two most plausible structures (Figure 7): **10A**$^+$, in which the Cu^I center is chelated by the free nitrogen atoms of the oxanMe ligand and a bridging acetate, and **10B**$^+$, which features a dative Pt→Cu bond supported by two acetate bridges, resulting in a slightly distorted T-shaped tricoordinate environment around the Cu^I center. The Pt→Cu bond in **10B**$^+$ (2.731 Å) is markedly longer than that found in the related complex {[(NN)PtMe$_2$]Cu(OTf)} [2.399 Å, NN = 2,3-bis(2,6-dichlorophenylimino)butane],[27] which is likely caused by the fact that acetate ligands are weaker σ-donors than methyl groups, resulting in reduced Lewis basicity of the platinum center. Structure **10B**$^+$ was found to be more stable than **10A**$^+$ by 10.6 kcal/mol and is thus the preferred structure of **10**$^+$ in the gas phase.

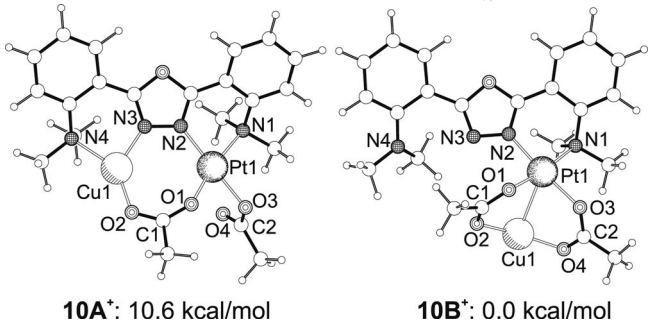

Figure 7. Calculated structures and relative energies for cation **10**$^+$. Selected distances [Å], angles [°], and torsion angles [°] for **10A**$^+$: Pt1–N1 2.145, Pt1–N2 2.018, Pt1–O1 2.082, Pt1–O3 2.083, Pt1–Cu1 3.743, Cu1–N3 1.958, Cu1–N4 2.146, Cu1–O2 1.877, N1–Pt1–N2 84.8, N3–Cu1–N4 88.2, N2–Pt1–O1 101.6, O1–Pt1–O3 78.8, Pt1–O1–C1 142.4, Cu1–O2–C1 125.9, Pt1–O3–C2 115.3, Pt1–N2–N3–Cu1 22.5; for **10B**$^+$: Pt1–N1 2.159, Pt1–N2 2.004, Pt1–O1 2.079, Pt1–O3 2.079, Pt1–Cu1 2.731, Cu1–O2 1.885, Cu1–O4 1.886, N1–Pt1–N2 86.6, N2–Pt1–O1 87.1, N1–Pt–O3 92.7, O1–Pt1–O3 93.0, O2–Cu–O4 156.3, Pt1–O1–C1 122.0, Pt1–O2–C2 124.2, Cu1–O2–C1 112.2, Cu1–O4–C2 113.6, Pt1–O1–C1–O2 19.6, Pt1–O3–C2–O4 –5.8, Cu1–O2–C1–O1 22.3, Cu1–O4–C2–O3 28.0.

A more detailed understanding of the reasons underlying the lower stability of **10A**$^+$ − which may appear surprising at first sight − is given by a close inspection of its geometry. The square-planar environment of the Pt^{II} center is distorted, with N2–Pt1–O1 and O1–Pt1–O2 angles of 101.6 and 78.8°, respectively, and the Pt1–O1–C1 angle of 142.4° is wider than the ideal value of ca. 120°. Furthermore, the Pt1–N2–N3–Cu1 dihedral angle (22.5°) is large, indicating suboptimal coordination of the oxadiazole bridge to the metals. Thus, structure **10A**$^+$ is highly strained, indicating that ligand **2** is presumably not suited for preparing dinuclear complexes incorporating planar 1,3-bridging ligands and a square-planar metal center.

The interaction of **9** with copper(I) was also studied in solution by ^{1}H NMR spectroscopy. Upon addition of one equivalent of [Cu(NCMe)$_4$]BArF to a solution of **9** in CD_2Cl_2, the resonances corresponding to the acetate ligands undergo a slight downfield shift from δ = 1.94 and 2.00 ppm to δ = 2.06 and 2.11 ppm, but the signal of the uncoordinated NMe_2 moiety is not affected. Thus, we infer that a, presumably acetonitrile solvated, salt of **10B**$^+$ (**10**-BArF) exists in solution (Scheme 3).

Attempts to isolate **10**$^+$ with a range of counterions (PF_6^-, ClO_4^-, $BArF^-$) failed due to its instability in solution. When a solution of **10**-BArF was stored for several hours at room temperature, a black precipitate (presumably Cu^0) forms. The concomitant appearance of a few very broad resonances in the ^{1}H NMR spectrum indicates the formation of a paramagnetic Cu^{II} species by disproportionation of Cu^I. ESI-MS analysis (Figure 6) shows the appearance of a new peak at *m*/*z* = 653, which is identified as the Cu^{II} complex [(oxanMe)$_2$Pt$_2$(OAc)$_4$Cu]$^{2+}$ (**11**$^{2+}$) on the basis of its isotope pattern. Upon CID, dication **11**$^{2+}$ cleanly fragments into two monocations of formula [(oxanMe)Pt(OAc)]$^+$ and [(oxanMe)Pt(OAc)$_3$Cu]$^+$, confirming its assignment.

In contrast to $\mathbf{10}^{+}$, dication $\mathbf{11}^{2+}$ could be isolated and crystallized as its $BArF^{-}$ salt. The XRD crystal structure of **11**-BArF (Figure 8) shows that $\mathbf{11}^{2+}$ has a centrosymmetrical structure in which the central Cu^{II} atom is encapsulated by two [(oxanMe)Pt(OAc)$_2$] units, forming a linear Pt^{II}–Cu^{II}–Pt^{II} chain. The copper center experiences an apically distorted octahedral environment with four short Cu–O bonds [1.942(3) and 1.960(3) Å] in the equatorial plane and two Pt→Cu dative bonds (Pt–Cu 2.7506 Å) in apical positions. There is precedence for Pt^{II}→Cu^{II} dative bonds supported by 1,3-bridging nucleobases,[32–34] including a similar Pt^{II}–Cu^{II}–Pt^{II} chain with 1-methyluracilate and 1-methylcytosine as bridging ligands.[35] Additionally, compounds exhibiting acetate-supported Pt–Hg bonds are known.[36] However, to the best of our knowledge, the carboxylate-bridged Pt^{II}–Cu^{II}–Pt^{II} motif found in **11**-BArF is unprecedented.

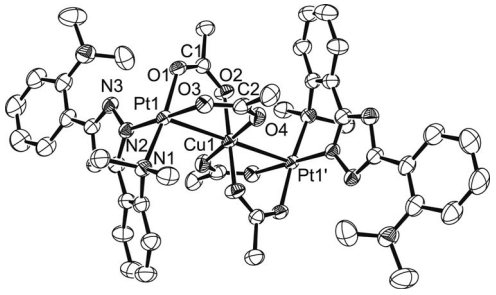

Figure 8. ORTEP representation of the centrosymmetric dication of **11**-BArF. Ellipsoids are drawn at 50% probability. For clarity, the two BArF counterions and a disordered diethyl ether molecule are omitted. Selected distances [Å] and angles [°]: Pt1–N1 2.087(4), Pt1–N2 1.975(4), Pt1–O1 2.007(3), Pt1–O3 2.019(3), Pt1–Cu1 2.7506(5), Cu1–O2 1.942(3), Cu1–O4 1.960(3), C1–O1 1.271(5), C1–O2 1.258(5), C2–O3 1.272(6), C2–O4 1.245(5), N1–Pt1–N3 87.65(14), N1–Pt1–O3 92.95(14), N2–Pt1–O1 91.26(13), O1–Pt1–O2 88.13(13), Pt1–O1–C1 125.1(3), Pt1–O3–C2 123.7(3), O2–Cu1–O4 91.38(14), O2–Cu1–O4′ 88.63(14), Cu1–O2–C1 123.4(3), Cu1–O4–C2 124.9(3).

Conclusions

The novel ligand oxanMe (**2**) was synthesized by methylation of the known oxan (**1**). The oxanMe ligand can be used to synthesize mononuclear complexes with common platinum(II) fragments, but it acts as a bis(bidentate) ligand in the tetranuclear copper(I) complex [(oxanMe)$_2$Cu$_4$Br$_4$] (**4**). The tendency of **2** to form mononuclear species is presumably due to the fact that coordination of a metal inductively removes electron density from the − already electron-poor − oxadiazole ring, making it weakly coordinating toward the second metal. In the reaction of diacetato complex **4** with [Cu(NCMe)$_4$]BArF, we observed the unexpected formation of a trinuclear complex that exhibits a Pt^{II}–Cu^{II}–Pt^{II} chain consisting of two Pt^{II}→Cu^{II} dative bonds supported by two acetate bridges each. Although no stable heterobinuclear complexes were obtained, the empty pocket of the mononuclear complexes could in principle be used to stabilize bimetallic intermediates in a catalytic cycle. This concept is currently investigated in our group.

Experimental Section

General: Solvents were obtained commercially in p.a. quality and used as received. For reactions involving metal complexes, solvents were distilled under an atmosphere of nitrogen over sodium (hexane, toluene), Na/K alloy (diethyl ether), potassium (tetrahydrofuran), or CaH_2 (acetonitrile, dichloromethane). All chemical manipulations involving metal complexes were performed under an inert atmosphere by using standard Schlenk and glove box techniques unless otherwise stated. ^{1}H and ^{13}C NMR spectra were recorded with Varian Gemini 300 and Varian Mercury 300 instruments. ^{1}H and ^{13}C chemical shifts are reported in ppm relative to tetramethylsilane, using residual solvent proton and ^{13}C resonances as internal references. Apparent singlets, doublets, and triplets are indicated by "s", "d", and "t", respectively. Elemental analyses were carried out by the Mikrolabor of the Laboratorium für Organische Chemie of ETH Zürich. Melting points are uncorrected and were measured in unsealed capillaries. Organolithium reagents were titrated by using the procedure of Watson and Eastham.[37] OxanH[28] (**1**), [Pt$_2$(CH$_3$)$_4$(μ-Me$_2$S)$_2$],[38] [(Me$_2$S)$_2$Pt(Me)Cl],[38] (PhCN)$_2$PtCl$_2$,[39] Na[BArF],[40] and [Cu(NCMe)$_4$][ClO$_4$],[41] were prepared according to literature procedures. All other chemicals were obtained commercially and used as received.

2,5-Bis[2-(dimethylamino)phenyl]-1,3,4-oxadiazole (oxanMe, 2): A suspension of $NaBH_4$ (2.2 g, 58 mmol) and **1** (1.01 g, 4 mmol) in THF (50 mL) was added over 30 min to a cooled mixture of formaldehyde (37% in water, 4 mL, 53 mmol), H_2SO_4 (3 M, 6.7 mL, 1 mmol), and THF (20 mL), resulting in a yellow suspension. Water (30 mL) was added, resulting in phase separation, followed by sodium carbonate until the pH of the water phase was distinctly basic. The organic phase was decanted, the water phase extracted with DCM (40 + 2 × 20 mL). The combined organic extract was washed with brine (30 mL), dried with $MgSO_4$, and concentrated under reduced pressure to yield a yellow solid. This residue was purified by column chromatography (110 g of silica, 1:3 ethyl acetate/petroleum ether containing 3% triethylamine) to yield a slightly yellow solid (1.04 g, 85%). M.p. 112–115 °C. ^{1}H NMR (300 MHz, [D$_6$]DMSO): δ = 7.74 (dd, $^3J_{H,H}$ = 7.7 Hz, $^5J_{H,H}$ = 1.7 Hz, 2 H, ArH^6), 7.50 (ddd, $^3J_{H,H}$ = 8.4 Hz, $^3J_{H,H}$ = 7.3 Hz, $^5J_{H,H}$ = 1.7 Hz, 2 H, ArH^4), 7.18 (dd, $^3J_{H,H}$ = 8.4 Hz, $^5J_{H,H}$ = 0.9 Hz, 2 H, ArH^3), 7.06 ("t"d, $^3J_{H,H}$ = 7.5 Hz, $^5J_{H,H}$ = 1.1 Hz, 2 H, ArH^5), 2.70 [s, 12 H, N(CH$_3$)$_2$] ppm. ^{13}C{^{1}H} NMR (75 MHz, [D$_6$]DMSO): δ = 164.2, 152.2, 132.3, 131.3, 120.4, 118.2, 114.9 (7 C_{Ar}), 43.3 (CH_3) ppm. $C_{18}H_{20}N_4O$ (308.38): calcd. C 70.11, H 6.54, N 18.17; found C 69.85, H 6.63, N 18.24.

Reaction of 2 with [Pt$_2$Me$_4$(μ-SMe$_2$)$_2$]: CD_2Cl_2 (0.7 mL) was added to a mixture of **2** (6.1 mg, 20 μmol) and [Pt$_2$Me$_4$(μ-SMe$_2$)$_2$] (5.7 mg, 10 μmol), resulting in a yellow solution that was left standing for 30 min. ^{1}H NMR analysis showed that the mixture contained **2** (45%), **3** (24%), [Pt$_2$Me$_4$(μ-SMe$_2$)$_2$] (12%), and [PtMe$_2$(SMe$_2$)$_2$] (19%), indicating a conversion rate of 35% based on the amount of **2**. Further standing at room temperature did not result in higher conversion, but slow decomposition was observed instead, leading to an intractable mixture of products over several hours. ^{1}H NMR (300 MHz, CD_2Cl_2): Only the signals of novel complex **3** are reported. The signals marked with * suffer from partial overlap with signals of **2**. δ = 7.93 (dd, $^3J_{H,H}$ = 7.6 Hz, $^5J_{H,H}$ = 1.7 Hz, 1 H, ArH^6), 7.92 (dd, $^3J_{H,H}$ = 7.9 Hz, $^5J_{H,H}$ = 1.7 Hz, 1 H, ArH^6), 7.64 (ddd, $^3J_{H,H}$ = 8.6 Hz, $^3J_{H,H}$ = 7.3 Hz, $^5J_{H,H}$ = 1.7 Hz, 1 H, ArH^4),

7.51* (ddd, $^3J_{H,H}$ = 8.5 Hz, $^3J_{H,H}$ = 7.1 Hz, $^5J_{H,H}$ = 1.7 Hz, 1 H, Ar*H*^{4}), 7.41* (dd, $^3J_{H,H}$ hidden, $^5J_{H,H}$ = 0.7 Hz, 1 H, Ar*H*^{3}), 7.35 ("t"d, $^3J_{H,H}$ = 7.6 Hz, $^5J_{H,H}$ = 0.9 Hz, 1 H, Ar*H*^{5}), 7.18 (dd, $^3J_{H,H}$ = 8.3 Hz, $^5J_{H,H}$ = 0.7 Hz, 1 H, Ar*H*^{3}), 7.07* ("t"d, $^3J_{H,H}$ = 7.6 Hz, $^5J_{H,H}$ = 1.1 Hz, 1 H, Ar*H*^{5}), 3.08 [s, $^3J_{H,Pt}$ = 14.0 Hz, 3 H, PtN(C*H*$_3$)$_2$], 2.85 [s, 3 H, N(C*H*$_3$)$_2$], 0.85 (s, $^2J_{H,Pt}$ = 94.6 Hz, 3 H, PtC*H*$_3$), 0.56 (s, $^2J_{H,Pt}$ = 85.5 Hz, 3 H, PtC*H*$_3$).

[(oxanMe)$_2$Cu$_4$Br$_4$] (4): CuBr (29 mg, 0.2 mmol) was added to a mixture of **2** (62 mg, 0.2 mmol) and [Pt$_2$(CH$_3$)$_4$(μ-Me$_2$S)$_2$] (58 mg, 0.1 mmol) in DCM (3 mL), and the solution was stirred for 0.5 h, during which time a small quantity of yellow needles formed. The orange solution was concentrated to ca. 1 mL and diethyl ether (4 mL) was added slowly while stirring. Filtration, washing of the solid with diethyl ether (3 × 1 mL), and drying in vacuo yielded the product as a yellow powder. ^{1}H NMR (300 MHz, CD_2Cl_2): δ = 8.00 (dd, $^3J_{H,H}$ = 7.9 Hz, $^5J_{H,H}$ = 1.6 Hz, 2 H, Ar*H*^{6}), 7.60 (ddd, $^3J_{H,H}$ = 8.4 Hz, $^3J_{H,H}$ = 7.3 Hz, $^5J_{H,H}$ = 1.7 Hz, 2 H, Ar*H*^{4}), 7.37 (dd, $^3J_{H,H}$ = 8.4 Hz, $^5J_{H,H}$ = 0.9 Hz, 2 H, Ar*H*^{3}), 7.25 (ddd, $^3J_{H,H}$ = 7.9 Hz, $^3J_{H,H}$ = 7.4 Hz, $^5J_{H,H}$ = 1.1 Hz, 2 H, Ar*H*^{5}), 2.88 (s, 12 H, C*H*$_3$) ppm. No ^{13}C NMR could be obtained due to poor solubility in DCM. $C_{36}H_{40}Br_4Cu_4N_8O_2$ (1190.56): calcd. C 36.32, H 3.39, N 9.41; found C 36.43, H 3.61, N 9.28. Crystals suitable for XRD analysis were obtained by vapor diffusion of diethyl ether into a dichloromethane solution of **4** at 4 °C.

[(oxanMe)Pt(Me)Cl] (5): This reaction was performed without protection from air. OxanMe (165 mg, 0.53 mmol) and *trans*-[PtMeCl(SMe$_2$)$_2$] were dissolved in THF (5 mL). The flask was placed in an 85 °C oil bath and boiled to almost dryness (ca. 10 min) The oily residue was dissolved again in THF (5 mL), and this cycle was repeated 15 times. The brown residue was dissolved in DCM (1 mL), treated with activated charcoal and filtered. Diethyl ether (ca. 2 mL) was added until persistent turbidity of the solution. After cooling at 4 °C for 1 h, an oily, brown precipitate was removed from the orange solution by decantation. The solvent was evaporated in vacuo, and the residue was dissolved in a minimal amount of DCM. Diethyl ether (ca. 3 mL) was added until persistent turbidity of the solution. The latter was stored at –20 °C overnight, during which time the product crystallized. Decantation of the solvent, washing with diethyl ether (3 × 1 mL) and drying in vacuo yielded the product as orange nodules (140 mg, 48%). An analytically pure sample was obtained by recrystallization from DCM/octane. ^{1}H NMR (300 MHz, $CDCl_3$): δ = 7.92 (dd, $^3J_{H,H}$ = 7.7 Hz, $^5J_{H,H}$ = 1.6 Hz, 2 H, Ar*H*^{6}), 7.91 (dd, $^3J_{H,H}$ = 7.9 Hz, $^5J_{H,H}$ = 1.7 Hz, 2 H, Ar*H*^{6}), 7.68 (ddd, $^3J_{H,H}$ = 8.5 Hz, $^3J_{H,H}$ = 7.4 Hz, $^5J_{H,H}$ = 1.7 Hz, 1 H, Ar*H*^{4}), 7.54–7.46 (m, 2 H, Ar*H*^{4,5}), 7.38 ("t"d, $^3J_{H,H}$ = 7.6 Hz, $^5J_{H,H}$ = 1.0 Hz, 1 H, Ar*H*^{5}), 7.16 (dd, $^3J_{H,H}$ = 8.4 Hz, $^5J_{H,H}$ = 0.9 Hz, 1 H, Ar*H*^{3}), 7.06 (ddd, $^3J_{H,H}$ = 7.9 Hz, $^3J_{H,H}$ = 7.3 Hz, $^5J_{H,H}$ = 1.1 Hz, 1 H, Ar*H*^{5}), 3.15 [br. s, $^3J_{H,Pt}$ not resolved, 6 H, PtN(C*H*$_3$)$_2$], 2.87 [s, 6 H, N(C*H*$_3$)$_2$], 1.38 (s, $^2J_{H,Pt}$ = 83.5 Hz, 3 H, PtC*H*$_3$) ppm. ^{13}C{^{1}H} NMR (75 MHz, $CDCl_3$): δ = 163.8, 158.9, 153.2, 151.2, 133.8, 133.5, 131.3, 129.4, 126.5, 120.7, 119.8, 118.7, 116.8, 112.7 (14 C^{Ar}), 51.0 [PtN(*C*H$_3$)$_2$], 44.3 [N(*C*H$_3$)$_2$], –22.7 (Pt*C*H$_3$), no $J_{C,Pt}$ observed ppm. $C_{19}H_{23}ClN_4OPt$ (553.95): calcd. C 41.20, H 4.18, N 10.11; found C 40.96, H 4.38, N 10.04. Crystals suitable for XRD analysis were obtained by dissolving **5** in a minimal amount of DCM, adding ten volumes of diethyl ether and letting the suspension stand for 3 d.

Reaction of 5 with [Cu(NCMe)$_4$][PF$_6$]: CD_2Cl_2 (0.7 mL) was added to **5** (11 mg, 20 μmol) and [Cu(NCMe)$_4$][PF$_6$] (7 mg, 19 μmol). After 30 min, the yellow suspension was filtered into an NMR tube and subjected to ^{1}H NMR and ESI-MS analysis, which showed that [(oxanMe)PtMe(NCMe)][PF$_6$] (**6**) was cleanly formed. ^{1}H NMR (300 MHz, CD_2Cl_2): δ = 8.01 (dd, $^3J_{H,H}$ = 7.7 Hz, $^5J_{H,H}$ = 1.6 Hz, 1 H, Ar*H*^{6}), 7.95 (dd, $^3J_{H,H}$ = 7.9 Hz, $^5J_{H,H}$ = 1.7 Hz, 1 H, Ar*H*^{6}), 7.82 ("t"d, $^3J_{H,H}$ = 7.7 Hz, $^5J_{H,H}$ = 1.5 Hz, 1 H, Ar*H*^{4}), 7.65 (d, $^3J_{H,H}$ = 8.4 Hz, 1 H, Ar*H*^{3}), 7.58 ("t"d, $^3J_{H,H}$ = 7.8 Hz, $^5J_{H,H}$ = 1.6 Hz, 1 H, Ar*H*^{4}), 7.54 ("t", $^3J_{H,H}$ = 7.6 Hz, 1 H, Ar*H*^{5}), 7.24 (d, $^3J_{H,H}$ = 8.0 Hz, 1 H, Ar*H*^{3}), 7.12 ("t", $^3J_{H,H}$ = 7.6 Hz, 1 H, Ar*H*^{5}), 3.20 [br. s, $^3J_{H,Pt}$ not resolved, 6 H, PtN(C*H*$_3$)$_2$], 2.87 [s, 6 H, N(C*H*$_3$)$_2$], 2.56 (s, $^3J_{H,Pt}$ = 12.9 Hz, 3 H, C*H*$_3$CNPt), 1.20 (s, $^3J_{H,Pt}$ = 80.1 Hz, 3 H, PtC*H*$_3$) ppm. MS (ESI+, DCM): *m*/*z* = 559 [M]$^+$.

[(oxanMe)PtCl$_2$] (7): A mixture of oxanMe (594 mg, 1.94 mmol) and [(PhCN)$_2$PtCl$_2$] (915 mg, 1.94 mmol) in THF (20 mL) was heated at reflux for 68 h. After cooling to room temperature, the precipitate was collected by filtration, washed with THF (3 × 3 mL), and dried in vacuo to afford 924 mg (1.62 mmol, 83%) of a yellow powder. ^{1}H NMR (300 MHz, CD_2Cl_2): δ = 8.04 (dd, $^3J_{H,H}$ = 7.6 Hz, $^5J_{H,H}$ = 1.7 Hz, 1 H, Ar*H*^{6}), 7.95 (dd, $^3J_{H,H}$ = 7.9 Hz, $^5J_{H,H}$ = 1.7 Hz, 1 H, Ar*H*^{6}), 7.77 (ddd, $^3J_{H,H}$ = 8.7 Hz, $^3J_{H,H}$ = 7.4 Hz, $^5J_{H,H}$ = 1.7 Hz, 1 H, Ar*H*^{4}), 7.62–7.50 (m, 3 H, Ar*H*^{3,4,5}), 7.20 (dd, $^3J_{H,H}$ = 8.5 Hz, $^5J_{H,H}$ = 0.7 Hz, 1 H, Ar*H*^{3}), 7.08 (ddd, $^3J_{H,H}$ = 7.9 Hz, $^3J_{H,H}$ = 7.3 Hz, $^5J_{H,H}$ = 1.0 Hz 1 H, Ar*H*^{5}), 3.29 [s, $^3J_{H,Pt}$ = 26.5 Hz (br. Pt satellites), 6 H, PtN(C*H*$_3$)$_2$] 2.90 [s, 6 H, N(C*H*$_3$)$_2$] ppm. ^{13}C{^{1}H} NMR (75 MHz, CD_2Cl_2): δ = 165.1, 158.2, 153.8, 150.4, 135.3, 134.1, 131.7, 130.4, 128.5, 120.7, 119.5, 118.9, 116.5, 112.0 (14 C_{Ar}), 55.9 [PtN(*C*H$_3$)$_2$], 44.3 [N(*C*H$_3$)$_2$] ppm. MS (ESI+, MeCN, AgOTf): *m*/*z* = 580 [M – Cl$^-$ + MeCN]$^+$. MS–MS (+580): *m*/*z* = 543 [580 – HCl], 739 [580 – MeCN], 502 [580 – MeCN – HCl]. $C_{18}H_{20}Cl_2N_4OPt$ (574.37): calcd. C 37.64, H 3.51, N 9.75; found C 37.31, H 3.55, N 9.37. Crystals suitable for XRD analysis were grown by slow concentration of a solution of **7** in MeCN (polymorph **A**) or by vapor diffusion of diethyl ether into a solution of **7** in dichloromethane (polymorph **B**).

***trans*-[(oxanMe)$_2$PtCl$_2$] (8):** After collection of **7** by filtration from the reaction described above, the filtrate was stored at room temperature for 3 d, during which time **8** crystallized as thin, pale-yellow needles containing 2 equiv. of THF (52 mg, ca. 5%). A solvent free sample was obtained by crystallization from MeCN. ^{1}H NMR (300 MHz, CD_2Cl_2): δ = 8.75 (dd, $^3J_{H,H}$ = 7.8 Hz, $^5J_{H,H}$ = 1.6 Hz, 1 H, Ar*H*^{6}), 7.84 (dd, $^3J_{H,H}$ = 8.0 Hz, $^5J_{H,H}$ = 1.5 Hz, 1 H, Ar*H*^{6}), 7.54 (ddd, $^3J_{H,H}$ = 8.5 Hz, $^3J_{H,H}$ = 7.3 Hz, $^5J_{H,H}$ = 1.7 Hz, 1 H, Ar*H*^{4}), 7.50 (ddd, $^3J_{H,H}$ = 8.4 Hz, $^3J_{H,H}$ = 7.3 Hz, $^5J_{H,H}$ = 1.7 Hz, 1 H, Ar*H*^{4}), 7.19 (dd, $^3J_{H,H}$ = 8.4 Hz, $^5J_{H,H}$ = 0.9 Hz, 1 H, Ar*H*^{3}), 7.09–6.95 (m, 3 H, Ar*H*^{3,5,5}), 2.86 [s, 6 H, N(C*H*$_3$)$_2$], 2.81 [s, 6 H, N(C*H*$_3$)$_2$] ppm. ^{13}C{^{1}H} NMR (75 MHz, CD_2Cl_2): δ = 165.6, 164.9, 154.1, 153.4, 134.2, 133.9, 133.8, 131.8, 121.2, 119.8, 119.3, 117.5, 114.0, 111.9 (14 C_{Ar}), 44.6, 43.5 [2 N(*C*H$_3$)$_2$] ppm. MS (ESI+, DCM): *m*/*z* = 883 (weak) [M + H]$^+$, +847 [M – Cl$^-$]$^+$. MS–MS (+883): *m*/*z* = 847 [883 – HCl]. MS–MS (+847): *m*/*z* = 810 [847 – HCl]. $C_{36}H_{40}Cl_2N_8O_2Pt$ (882.75): calcd. C 48.98, H 4.57, N 12.69; found C 48.69, H 4.75, N 12.52. Crystals suitable for XRD analysis were obtained by crystallization from hot MeCN.

[(oxanMe)Pt(OOCCH$_3$)$_2$] (9): A mixture of **7** (350 mg, 0.61 mmol) and silver acetate (204 mg, 1.22 mmol) in DCM (20 mL) was stirred for 20 h in the dark. Filtration and washing of the precipitate with DCM (2 × 2 mL) yielded a brown solution, from which the solvent was removed in vacuo to yield the product as a light-brown powder (366 mg, 96%). An analytically pure sample was obtained by slow crystallization from DCM/Et_2O. ^{1}H NMR (300 MHz, CD_2Cl_2): δ = 8.08 (dd, $^3J_{H,H}$ = 7.7 Hz, $^5J_{H,H}$ = 1.7 Hz, 1 H, Ar*H*^{6}), 7.90 (dd, $^3J_{H,H}$ = 7.9 Hz, $^5J_{H,H}$ = 1.7 Hz, 1 H, Ar*H*^{6}), 7.77 (ddd, $^3J_{H,H}$ = 8.6 Hz, $^3J_{H,H}$ = 7.4 Hz, $^5J_{H,H}$ = 1.7 Hz, 1 H,

ArH^4), 7.66 (dd, $^3J_{H,H}$ = 8.5 Hz, $^5J_{H,H}$ = 0.9 Hz, 1 H, ArH^3), 7.58 ("t"d, $^3J_{H,H}$ = 7.6 Hz, $^5J_{H,H}$ = 1.1 Hz, 1 H, ArH^5), 7.53 (ddd, $^3J_{H,H}$ = 8.5 Hz, $^3J_{H,H}$ = 7.3 Hz, $^5J_{H,H}$ = 1.7 Hz, 1 H, ArH^4), 7.20 (dd, $^3J_{H,H}$ = 8.4 Hz, $^5J_{H,H}$ = 0.9 Hz, ArH^3), 7.07 (ddd, $^3J_{H,H}$ = 8.2 Hz, $^3J_{H,H}$ = 7.4 Hz, $^5J_{H,H}$ = 1.1 Hz, 1 H, ArH^5), 3.27 [s (br., $^3J_{H,Pt}$ not resolved, 6 H, PtN(CH_3)$_2$], 2.85 [s, 6 H, N(CH_3)$_2$], 2.00 (s, 3 H, CH_3COO), 1.94 (s, 3 H, CH_3COO) ppm. ^{13}C{^{1}H} NMR (75 MHz, CD_2Cl_2): δ = 177.4, 177.3 [2 *C*(=O)O], 164.4, 156.7, 153.8, 149.9, 135.1, 134.0, 131.5, 130.0, 128.9, 120.9, 120.0, 119.1, 116.2, 112.6 (14 C_{Ar}), 55.5 [PtN(*C*H$_3$)$_2$], 44.3 [N(*C*H$_3$)$_2$], 23.5, 22.5 (2 H$_3$*C*COO) ppm. MS (ESI+, DCM): *m*/*z* = 562 [M – MeCOO$^-$]$^+$, 870 [M + oxanMe – MeCOO$^-$]$^+$, 1183 [2M – MeCOO$^-$]$^+$. MS–MS (+562): *m*/*z* = 502 [562 – MeCOOH]. MS–MS (+870): *m*/*z* = 562 [870 – oxanMe]. MS–MS (+1183): *m*/*z* = 562 {1183 – [(oxanMe)-Pt(OOCMe)$_2$]}. $C_{22}H_{26}N_4O_5Pt$ (621.55): calcd. C 42.51, H 4.22, N 9.01; found C 42.22, H 4.26, N 8.90. Crystals suitable for XRD analysis were obtained by vapor diffusion of diethyl ether into a dichloromethane solution of **9** at 4 °C.

{[(oxanMe)Pt(OOCCH$_3$)$_2$]$_2$Cu}{BArF}$_2$ (11-BArF): A mixture of [Cu(NCMe)$_4$]ClO$_4$ (83 mg, 0.25 mmol) and NaBArF (150 mg, 0.17 mmol) in diethyl ether (10 mL) was stirred for 35 min and filtered. The filtrate, containing [Cu(NCMe)$_4$]BArF,[42] was freed from solvent in vacuo and dissolved in DCM (3 mL). A solution of **9** (95 mg, 0.15 mmol) in DCM (7 mL) was slowly added, and the mixture was stirred for 1.5 h. The solvent was evaporated, and the solid residue was extracted with diethyl ether (5 + 2 mL). The solvent was evaporated, and the residue taken up in diethyl ether (5 mL) and freed from solvent in vacuo. The solid residue was then dissolved in DCM (8 mL), a dark solid (presumably Cu^0) was filtered off, and hexane was added until persistent turbidity. The mixture was cooled to –20 °C for 2 h, and the formed dark oil was removed by decantation. Further concentration, filtration, and drying in vacuo yielded the product as a mustard-yellow powder (90 mg, 0.03 mmol, 39% based on **9**). An analytically pure sample, containing one equivalent of solvent, was obtained by crystallization from diethyl ether. MS (ESI+, DCM): *m*/*z* = 653 [M]$^{2+}$, 562 [(oxanMe)Pt(OOCMe)]$^+$, 744 [(oxanMe)Pt(OOCMe)$_3$Cu]$^+$. MS–MS (+653): *m*/*z* = 562 [(oxanMe)Pt(OOCMe)]$^+$, 744 [(oxanMe)-Pt(OOCMe)$_3$Cu]$^+$. MS (ESI–, DCM): *m*/*z* = –863 [BArF]$^-$. $C_{108}H_{76}B_2CuF_{48}N_8O_{10}Pt_2{\cdot}C_4H_{10}O$ (3107.19): calcd. C 43.29, H 2.79, N 3.61; found C 43.28, H 2.77, N 3.65. Crystals suitable for XRD analysis were obtained from diethyl ether.

Reaction of 9 with [Cu(NCMe)$_4$]BArF: Compound **9** (17 μmol) was added to a freshly prepared solution of [Cu(NCMe)$_4$]BArF (17 μmol) in CD_2Cl_2 (0.7 mL), and the resulting solution was subjected to ^{1}H NMR analysis. ^{1}H NMR (300 MHz, CD_2Cl_2): δ = 8.15 (dd, $^3J_{H,H}$ = 7.7 Hz, $^5J_{H,H}$ = 1.6 Hz, 1 H, ArH^6), 7.93 (dd, $^3J_{H,H}$ = 7.9 Hz, $^5J_{H,H}$ = 1.6 Hz, 1 H, ArH^6), 7.90–7.50 (m, 4 H, Ar$H^{3,4,4,5}$), 7.72 (br. s, 8 H, BAr$H^{2,6}$), 7.56 (br. s, 4 H, BArH^4), 7.25 (d, $^3J_{H,H}$ = 8.5 Hz, ArH^3), 7.07 ("t"d, $^3J_{H,H}$ = 7.6 Hz, $^5J_{H,H}$ = 1.1 Hz, 1 H, ArH^5), 3.25 [br. s, $^3J_{H,Pt}$ not resolved, 6 H, PtN(CH_3)$_2$], 2.85 [s, 6 H, N(CH_3)$_2$], 2.11 (s, 3 H, CH_3COO), 2.06 (s, 3 H, CH_3COO), 1.97 (s, 12 H, NCCH_3) ppm.

Computational Methods: All DFT calculations were performed using Gaussian 03.[43] Geometry optimizations were performed using the BP86 functional. The SDD basis set and effective core potential were used for transition metals, along with a 6-31+G(d) basis set on all other atoms. A frequency calculation was performed on all converged geometries to verify that they were minima.

Crystallographic Data: Relevant details about the structure refinements are given in Tables 1 and 2, and selected geometrical parameters are included in the captions of the corresponding figures. Data collection was performed with a Bruker-Nonius Kappa-CCD (graphite monochromator, Mo-K_α). The structures were solved by direct methods[44] and refined by full-matrix least-squares analysis[45] including an isotropic extinction correction. All non H-atoms were refined anisotropically (H-atoms isotropically, whereby H-positions are based on stereochemical considerations). CCDC-729779 (for **7A**), -729780 (for **7B**), -729781 (for **9**), -729782 (for **8**), -729783

Table 1. Crystallographic data for compounds **4**, **5**, **7**, and **8**.

	4	**5**	**7A**	**7B**	**8**
Formula	$C_{40}H_{48}N_8O_2Cl_8Cu_4Br_4$	$C_{19}H_{23}N_4OClPt$	$C_{18}H_{20}N_4OCl_2Pt$	$C_{18}H_{20}N_4OCl_2Pt$	$C_{36}H_{40}N_8O_2Cl_2Pt$
Fw	1526.23	553.95	574.37	574.37	882.75
Cryst. syst.	monoclinic	orthorhombic	orthorhombic	monoclinic	monoclinic
Space group	*C*2/*c*	$P2_12_12_1$	$P2_12_12_1$	*C*2/*c*	*C*2/*c*
a [Å]	16.5611(9)	8.7523(2)	8.5356(2)	21.5110(6)	36.0153(6)
b [Å]	21.9832(10)	13.4873(3)	13.4192(3)	15.3857(4)	9.1396(2)
c [Å]	15.6790(8)	16.9174(4)	16.9765(4)	14.5491(4)	27.6811(7)
α [°]	90	90	90	90	90
β [°]	98.699(2)	90	90	125.751(1)	128.548(1)
γ [°]	90	90	90	90	90
V [Å^3]	5642.5(5)	1997.01(8)	1944.50(8)	3907.84(18)	7126.1(3)
Z	4	4	4	8	8
$D_{calcd.}$ [g/cm^3]	1.797	1.842	1.962	1.953	1.646
F(000)	2992	1072	1104	2208	3520
μ [1/mm]	4.739	7.175	7.506	7.469	4.133
Temp. [K]	180	220	220	220	173
Wavelength [Å]	0.7107	0.7107	0.7107	0.7107	0.7107
Measd. rflns.	11426	4534	4442	8702	13793
Unique rflns.	6370	2591	4442	4471	8076
Data/restr./param.	6370/0/295	2591/0/241	4442/0/251	4471/0/264	8076/0/451
R(F) [$I > 2\sigma(I)$]	0.0547	0.0374	0.0327	0.0384	0.0553
wR(F^2) [$I > 2\sigma(I)$]	0.1443	0.0991	0.0772	0.0952	0.1209
GOF	1.002	1.048	1.016	1.014	1.102

(for **4**), -729784 (for **5**), and -729785 (for **11**-BArF) contain the supplementary crystallographic data for this paper. These data can be obtained free of charge from The Cambridge Crystallographic Data Centre via www.ccdc.cam.ac.uk/data_request/cif.

Table 2. Crystallographic data for compounds **9** and **11**-BArF.

	9	**11**-BArF
Formula	$C_{48}H_{62}N_8O_{11}Pt_2$	$C_{116}H_{76}N_8O_{12}B_2F_{48}CuPt_2$
Fw	1317.24	3161.19
Cryst. syst.	triclinic	triclinic
Space group	$P\bar{1}$	$P\bar{1}$
a [Å]	12.9129(13)	13.1020(12)
b [Å]	14.1881(13)	13.1469(12)
c [Å]	15.3750(14)	19.773(2)
α [°]	107.069(12)	100.909(11)
β [°]	107.261(12)	102.815(12)
γ [°]	90.020(11)	97.414(10)
V [Å^3]	2559.7(5)	3208.6(6)
Z	2	1
$D_{calcd.}$ [g/cm^3]	1.709	1.636
F(000)	1300	1551
μ [1/mm]	5.525	2.468
Temp. [K]	220	200
Wavelength [Å]	0.7107	0.7107
Measd. rflns.	20890	24503
Unique rflns.	11758	14608
Data/restr./param.	11758/0/636	14608/0/829
$R(F)$ [$I>2\sigma(I)$]	0.0468	0.0446
$wR(F^2)$ [$I>2\sigma(I)$]	0.1111	0.1152
GOF	1.045	1.007

Acknowledgments

The authors acknowledge support from the Swiss National Foundation. We thank Mr. P. Seiler for the X-ray structure determinations.

[1] M. Lersch, M. Tilset, *Chem. Rev.* **2005**, *105*, 2471–2526.
[2] J. L. Garnett, R. J. Hodges, *J. Am. Chem. Soc.* **1967**, *89*, 4546–4547.
[3] J. P. Perdew, K. Burke, Y. Wang, *Phys. Rev. B* **1996**, *54*, 16533.
[4] S. Reinartz, P. S. White, M. Brookhart, J. L. Templeton, *J. Am. Chem. Soc.* **2001**, *123*, 12724–12725.
[5] K. J. H. Young, S. K. Meier, J. M. Gonzales, J. Oxgaard, W. A. Goddard III, R. A. Periana, *Organometallics* **2006**, *25*, 4734–4737.
[6] R. A. Periana, D. J. Taube, S. Gamble, H. Taube, T. Satoh, H. Fujii, *Science* **1998**, *280*, 560–564.
[7] H. C. Lo, A. Haskel, M. Kapon, E. Keinan, *J. Am. Chem. Soc.* **2002**, *124*, 3226–3228.
[8] D. D. Wick, K. I. Goldberg, *J. Am. Chem. Soc.* **1997**, *119*, 10235–10236.
[9] U. Fekl, K. I. Goldberg, *J. Am. Chem. Soc.* **2002**, *124*, 6804–6805.
[10] T. J. Williams, A. J. M. Caffyn, N. Hazari, P. F. Oblad, J. A. Labinger, J. E. Bercaw, *J. Am. Chem. Soc.* **2008**, *130*, 2418–2419.
[11] L. Johannsson, O. B. Ryan, M. Tilset, *J. Am. Chem. Soc.* **1999**, *121*, 1974–1975.
[12] S. M. Kloek, K. I. Goldberg, *J. Am. Chem. Soc.* **2007**, *129*, 3460–3461.
[13] B. Butschke, M. Schlangen, D. Schröder, H. Schwarz, *Helv. Chim. Acta* **2008**, *91*, 1902–1914.
[14] E. Khaskin, P. Y. Zavalij, A. N. Vedernikov, *J. Am. Chem. Soc.* **2006**, *128*, 13054–13055.
[15] C. M. Thomas, J. C. Peters, *Organometallics* **2005**, *24*, 5858–5867.
[16] H. A. Zhong, J. A. Labinger, J. E. Bercaw, *J. Am. Chem. Soc.* **2002**, *124*, 1378–1399.
[17] G. S. Chen, J. A. Labinger, J. E. Bercaw, *Proc. Natl. Acad. Sci. USA* **2007**, *104*, 6915–6920.
[18] C. N. Iverson, C. A. G. Carter, R. T. Baker, J. D. Scollard, J. A. Labinger, J. E. Bercaw, *J. Am. Chem. Soc.* **2003**, *125*, 12674–12675.
[19] D. Karshtedt, J. L. McBee, A. T. Bell, T. D. Tilley, *Organometallics* **2006**, *25*, 1801–1811.
[20] D. Song, W. L. Jia, S. Wang, *Organometallics* **2004**, *23*, 1194–1196.
[21] L. A. Hammad, G. Gerdes, P. Chen, *Organometallics* **2005**, *24*, 1907–1913.
[22] M.-E. Moret, P. Chen, *Organometallics* **2007**, *26*, 1523–1530.
[23] F. Zhang, C. W. Kirby, D. W. Hairsine, M. C. Jennings, R. J. Puddephatt, *J. Am. Chem. Soc.* **2005**, *127*, 14196–14197.
[24] G. Gerdes, P. Chen, *Organometallics* **2004**, *23*, 3031–3036.
[25] V. R. Ziatdinov, J. Oxgaard, O. A. Mironov, K. J. H. Young, W. A. Goddard III, R. A. Periana, *J. Am. Chem. Soc.* **2006**, *128*, 7404–7405.
[26] M.-E. Moret, P. Chen, *Organometallics* **2008**, *27*, 4903–4916.
[27] M.-E. Moret, P. Chen, *J. Am. Chem. Soc.* **2009**, *131*, 5675–5690.
[28] C. Incarvito, A. L. Rheingold, C. J. Qin, A. L. Gavrilova, B. Bosnich, *Inorg. Chem.* **2001**, *40*, 1386–1390.
[29] C. Incarvito, A. L. Rheingold, A. L. Gavrilova, C. Jin Quin, B. Bosnich, *Inorg. Chem.* **2001**, *40*, 4101–4108.
[30] A. G. Giumanini, G. Chiavari, M. M. Musiani, P. Rossi, *Synthesis* **1980**, *9*, 743–746.
[31] Y. E. Filinchuk, M. G. Myskiv, V. N. Davydov, *J. Struct. Chem.* **2000**, *41*, 851–857.
[32] D. Neugebauer, B. Lippert, *J. Am. Chem. Soc.* **1982**, *104*, 6596–6601.
[33] G. Fusch, E. C. Fusch, A. Erxleben, J. Hüttermann, H.-J. Scholl, B. Lippert, *Inorg. Chim. Acta* **1996**, *252*, 167–178.
[34] J. A. R. Navarro, E. Freisinger, B. Lippert, *Eur. J. Inorg. Chem.* **2000**, 147–151.
[35] B. Lippert, U. Thewalt, H. Schöllhorn, D. M. L. Goodgame, R. W. Rollins, *Inorg. Chem.* **1984**, *23*, 2807–2813.
[36] A. F. M. van der Ploeg, G. van Koten, K. Vrieze, A. L. Spek, A. J. M. Duisenberg, *J. Chem. Soc., Chem. Commun.* **1980**, 469–471.
[37] S. C. Watson, J. F. Eastham, *J. Organomet. Chem.* **1967**, *9*, 165–168.
[38] G. S. Hill, M. J. Irwin, C. J. Levy, L. M. Rendina, R. J. Puddephatt, *Inorg. Synth.* **1998**, *32*, 149–152.
[39] G. K. Anderson, M. Lin, *Inorg. Synth.* **1990**, *28*, 60–63.
[40] N. A. Yakelis, R. G. Bergman, *Organometallics* **2005**, *24*, 3579–3581.
[41] H.-C. Liang, K. D. Karlin, R. Dyson, S. Kaderli, B. Jung, A. D. Zuberbühler, *Inorg. Chem.* **2000**, *39*, 5884–5894.
[42] M.-A. Kopf, Y.-M. Neuhold, A. D. Zuberbühler, K. D. Karlin, *Inorg. Chem.* **1999**, *38*, 3093–3102.
[43] M. J. Frisch, G. W. Trucks, H. B. Schlegel, G. E. Scuseria, M. A. Robb, J. R. Cheeseman, J. A. Montgomery Jr., T. Vreven, K. N. Kudin, J. C. Burant, J. M. Millam, S. S. Iyengar, J. Tomasi, V. Barone, B. Mennucci, M. Cossi, G. Scalmani, N. Rega, G. A. Petersson, H. Nakatsuji, M. Hada, M. Ehara, K. Toyota, R. Fukuda, J. Hasegawa, M. Ishida, T. Nakajima, Y. Honda, O. Kitao, H. Nakai, M. Klene, X. Li, J. E. Knox, H. P. Hratchian, J. B. Cross, V. Bakken, C. Adamo, J. Jaramillo, R. Gomperts, R. E. Stratmann, O. Yazyev, A. J. Austin, R. Cammi, C. Pomelli, J. W. Ochterski, P. Y. Ayala, K. Morokuma, G. A. Voth, P. Salvador, J. J. Dannenberg, V. G. Zakrzewski, S. Dapprich, A. D. Daniels, M. C. Strain, O. Farkas, D. K. Malick, A. D. Rabuck, K. Raghavachari, J. B. Foresman, J. V. Ortiz, Q. Cui, A. G. Baboul, S. Clifford, J. Cioslowski, B. B. Stefanov, G. Liu, A. Liashenko, P. Piskorz, I. Komaromi, R. L.

Martin, D. J. Fox, T. Keith, M. A. Al-Laham, C. Y. Peng, A. Nanayakkara, M. Challacombe, P. M. W. Gill, B. Johnson, W. Chen, M. W. Wong, C. Gonzalez, J. A. Pople, *Gaussian 03*, Revision D.01, Gaussian, Inc., Wallingford, CT, **2004**.
[44] A. Altomare, M. Burla, M. Camalli, G. Cascarano, C. Giacovazzo, A. Guagliardi, A. Moliterni, G. Polidori, R. J. Spagna, *Appl. Crystallogr.* **1999**, *32*, 115–119.
[45] G. M. Sheldrick, *SHELXL-97 Program for the Refinement of Crystal Structures*, University of Göttingen, Germany, **1997**.
Received: September 8, 2009
Published Online: December 8, 2009

